Enhancing Grazing Incidence Sound Absorption in Three-Dimensional Printed Triply Periodic Minimal Surfaces through Geometric Asymmetry

Janith Godakawela[1], Anthony Ciletti[2], Bhisham Sharma[3]
Michigan Technological University
Houghton, MI 49931, USA

Martha C. Brown[4]
NASA Langley Research Center
Mail Stop 164D
Hampton, VA 23681, USA

ABSTRACT

Triply periodic minimal surfaces (TPMS) offer promising absorption performance due to their tunable geometry. Previous findings under normal incidence conditions show that introducing geometric asymmetry can enhance sound absorption without increasing overall density. This study investigates whether those improvements hold under grazing incidence conditions with and without flow, which are more representative of practical flow environments. TPMS samples are fabricated using fused deposition modeling, and their acoustic response is measured in the Grazing Flow Impedance Tube (GFIT) at NASA Langley Research Center. Results confirm that symmetry-breaking improves low-frequency absorption under grazing incidence, mirroring outcomes observed at normal incidence. These findings underscore the versatility of TPMS-based approaches for advanced noise mitigation while maintaining minimal mass. Overall, harnessing geometric asymmetry offers a powerful means to optimize performance across diverse incidence angles, laying the groundwork for lightweight, high-performance acoustic liners suitable for aerospace, automotive, and industrial applications.

1. INTRODUCTION

Mitigating unwanted noise is a critical challenge in sectors ranging from aerospace and automotive to urban infrastructure, where designers are increasingly searching for lightweight, multifunctional materials [1-3]. Traditional porous absorbers—often fabricated from fibrous or granular materials—have long been employed for noise control [4]. However, these conventional solutions typically suffer from a limited operational bandwidth and are designed for only sound absorption. A common method to enhance their performance is by reducing porosity, which increases density and viscous losses. However, this approach comes at a considerable cost: the additional mass can be prohibitive in applications where weight is a constraint. In contrast, recent innovations focus on novel geometries that improve energy dissipation without a corresponding weight penalty.

[1]pgodakaw@mtu.edu, Graduate Student, Mechanical and Aerospace Engineering
[2]avcilett@mtu.edu, Graduate Student, Mechanical and Aerospace Engineering
[3]bnsharma@mtu.edu, Associate Professor, Mechanical and Aerospace Engineering
[4]martha.c.brown@nasa.gov, Senior Research Engineer, Aeroacoustics Branch

Advances in additive manufacturing have been pivotal in enabling the fabrication of such intricate structures with high fidelity and reproducibility [5]. One promising class of materials developed through these techniques is based on Triply Periodic Minimal Surfaces (TPMS) [6]. These structures are characterized by continuous, highly interconnected networks and large specific surface areas that allow precise control over cell size, porosity, and wall thickness [7]. Rather than relying on a reduction in porosity, TPMS-based designs can be engineered through geometric manipulation to optimize energy dissipation [8, 9]. This approach enhances sound absorption while maintaining, or even reducing, the overall mass, thereby addressing a critical need in modern, high-performance systems.

Among the various TPMS configurations, the gyroid structure has attracted significant attention due to its unique geometrical features and its ease of manufacture using modern additive processes [10, 11]. Previous work demonstrated that introducing geometric asymmetry—specifically by elongating the unit cells along one axis—could significantly enhance sound absorption under normal incidence conditions [12]. Normal incidence experiments showed that elongation increases the magnitude of the absorption peaks, shifts these peaks to lower frequencies, and narrows the width when compared with base gyroid structures. These observations suggest that controlled manipulation of the internal geometry can optimize viscous losses and internal reflections, thereby enhancing energy dissipation without incurring the weight penalties of simply reducing porosity.

While the enhancements observed under normal incidence provide a promising foundation, they represent only one aspect of the overall acoustic performance. In practical applications, sound waves rarely impinge perpendicularly on a surface. Instead, devices such as acoustic liners in aircraft engines, automotive exhaust systems, and industrial noise barriers are typically exposed to oblique or grazing sound incidence, often in the presence of flow [13]. This discrepancy between idealized laboratory conditions and real-world scenarios underscores the necessity of extending our investigations beyond normal incidence. The present study, therefore, focuses on evaluating the acoustic performance of elongated gyroid TPMS structures under grazing incidence conditions using a Grazing Flow Impedance Tube (GFIT).

The GFIT apparatus allows us to simulate realistic operating environments by introducing controlled airflow and mimicking the grazing incidence of sound waves. This experimental setup provides a more comprehensive understanding of how the benefits of geometric asymmetry observed under normal incidence translate into grazing flow conditions. By comparing the grazing incidence data with our earlier normal incidence results, we aim to determine whether the improvements in absorption—such as enhanced peak magnitudes and frequency shifts—are maintained or further modified when the absorber is subjected to grazing sound incidence and flow effects.

In summary, this study aims to bridge the gap between the idealized acoustic performance of TPMS absorbers under normal incidence and the complex realities of aeroacoustic, real-world environments. By leveraging advances in additive manufacturing to produce intricate gyroid structures with controlled geometric asymmetry and by systematically evaluating their performance under both no-flow and flow conditions, we seek to develop a deeper understanding of how multifunctional materials can be engineered for next-generation acoustic applications. The insights gained have the potential to inform the design of lightweight, high-performance acoustic liners that meet the stringent requirements of modern aerospace, automotive, and industrial systems.

2. SAMPLE FABRICATION AND MEASUREMENT

This study specifically investigates elongated gyroid-based TPMS structures. The gyroid geometry is mathematically described by the implicit equation

$$\left(sin\left(\frac{2\pi}{a_x}x\right)cos\left(\frac{2\pi}{a_y}y\right)+sin\left(\frac{2\pi}{a_y}y\right)cos\left(\frac{2\pi}{a_z}z\right)+sin\left(\frac{2\pi}{a_z}z\right)cos\left(\frac{2\pi}{a_x}x\right)\right)^2-c^2=0, \qquad (1)$$

where x, y, and z represent Cartesian coordinates, parameters a_x, a_y, and a_z control the side length of the unit cells in x, y, and z directions, respectively, and parameter c determines the relative density (ρ) of the structure. When $c = 0$, the resulting geometry is a surface without thickness, as illustrated in Figure 1(a). Assigning a non-zero value to c produces a thickened structure, adding volume to the TPMS surface, as shown in Figure 1(b).

To induce geometric asymmetry, the unit cells are elongated along the x-axis. This elongation is implemented by selectively increasing the unit cell dimension parameter in the x-direction (a_x), while maintaining constant dimensions in the y and z directions. The base gyroid unit cell measures 5 mm per side. Three elongation factors of 2, 3, and 4 were investigated, corresponding to elongated unit cell lengths of 10 mm, 15 mm, and 20 mm, respectively. To compensate for density reductions caused by elongation, the wall thickness was incrementally adjusted, ensuring a consistent design relative density of 40% across all samples. Samples are systematically labeled using the notation “GYREX#,” where "GYR" denotes the gyroid structure, "E" indicates elongation, "X" specifies the elongation axis (x-axis), and "#" represents the elongation factor. For instance, "GYREX3" refers to a gyroid structure elongated by a factor of 3 along the x-axis (Figure 1(c)).

All samples were fabricated as rectangular prisms measuring 25.4 mm in thickness, 63.5 mm in width, and 41.529 cm in length, with an additional 6.35 mm border to facilitate mounting onto the test fixture. Samples were designed with their elongation axis aligned along the sample's length. Structures were designed using an implicit modeling approach within nTopology software and subsequently processed through IdeaMaker slicing software, employing a layer height of 0.15 mm. Printing was conducted using a Modi3d Big Meter fused filament fabrication (FFF) printer equipped with a 0.4 mm nozzle and polylactic acid (PLA) filament of 1.75 mm diameter. Printing parameters included a nozzle temperature of 205°C and 100% infill in the active sample region to ensure structural robustness. Due to the substantial print times—approximately six days per sample—the sample thickness was limited to 25.4 mm.

Normal incidence acoustic absorption was characterized using the Mecanum 38.1 mm square impedance tube with a two-microphone configuration following ASTM E1050-19 standards [14]. Acoustic excitation was provided by a low-distortion audio amplifier driving a loudspeaker at one end of the impedance tube, with the sample positioned flush against a rigid backing at the other end without an air gap. Incident and reflected pressures were captured using two PCB 130F22 TEDS microphones, maintaining a consistent input sound pressure level (SPL) of 90 dB. Environmental parameters such as temperature, pressure, and humidity were recorded using the Mecanum Enviro weather station.

Each sample underwent testing with the elongation axis in perpendicular orientation to the direction of sound propagation. Acoustic measurements consisted of five replicates, each with 150 averages to minimize measurement noise, across a frequency range of 115–4300 Hz. The transfer function, H_{12},

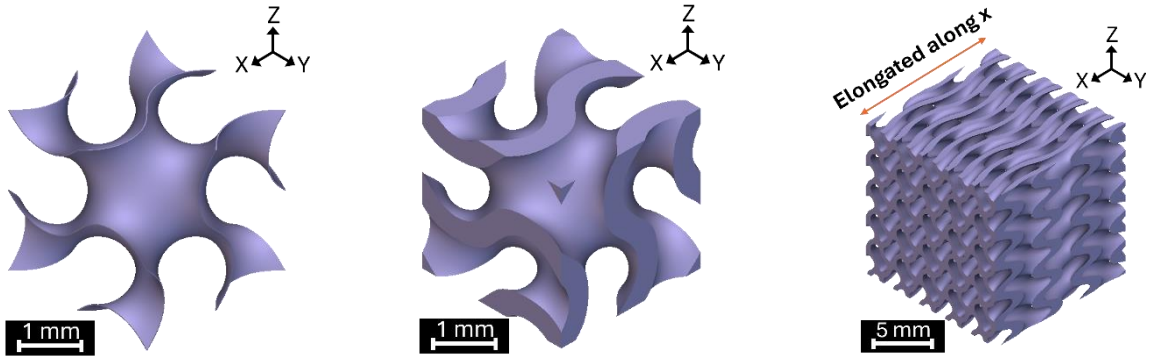

(a) (b) (c)

Figure 1: Representative geometries of (a) gyroid surface unit cell, (b) thickened gyroid unit cell, and (c) elongated gyroid

between the microphones was measured using Mecanum Tube-x software, enabling calculation of the reflection coefficient, *R*, according to

$$R = \frac{H_{12} - e^{-jks}}{e^{jks} - H_{12}} e^{j2k(l+s)}, \quad (2)$$

where *k* is the wave number in air, *j* is the imaginary unit, *s* represents microphone spacing, and *l* is the distance from the reference microphone to the sample surface. Subsequently, the normal incidence sound absorption coefficient, α, was determined as

$$\alpha = 1 - |R|^2. \quad (3)$$

Grazing incidence testing was performed at the Grazing Flow Impedance Tube (GFIT) at the NASA Langley Research Center. GFIT is a 50.8 mm by 63.5 mm waveguide that evaluates the acoustic performance of a liner in an aeroacoustic environment that mimics the conditions of an aft-bypass duct. The flow path consists of a straight duct with an upstream acoustic source section using 12 drivers, interchangeable lengths of blank duct, a test section where the installed liner sample is located on the upper wall of the duct, and an array of 95 measurement microphones leading to a 12-driver downstream source section. Near-anechoic terminating diffusers are situated at the end of the duct to control reflections and reduce overall flow noise. The source sections generate sound pressure levels up to 150 dB for a frequency range between 400 and 3000 Hz. Grazing flow conditions from Mach 0.0 to Mach 0.6 are available with such an arrangement [13]. For this preliminary study, only Mach 0.3 is investigated. The data are acquired in a modified swept-sine process, developed at NASA Langley [15].

Grazing incidence tests were conducted using the GFIT setup under three configurations. All samples were designed with their elongation axis oriented along the sample length, ensuring alignment parallel to the longitudinal axis of the GFIT. This orientation was selected based on insights from prior studies on normal incidence sound absorption. In the first configuration, the samples were directly mounted onto a 6.35 mm aluminum backing plate without airflow. The second configuration included a wire mesh as a facesheet with a constant resistance of 3 cgs Rayl inserted between the sample and the tube, again without airflow. The wire mesh was selected because the acoustic performance is independent of SPL, and it improves flow quality. The third configuration involved the addition of grazing airflow at Mach 0.3 with a wire mesh facesheet and back plate setup. Each test condition was performed at three SPL levels—120, 130, and 140 dB—to confirm acoustic linearity, meaning that the acoustic performance is independent on SPL. Table 1 summarizes the test configurations explored in this study. Although this

Table 1: Test matrix

Sample Name	Elongation Factor	Facesheet	Mach number	Source SPL (dB)
GYREX1	1	None	0.0	120, 130, 140
GYREX1	1	None	0.0	120, 130, 140
GYREX1	1	3cgs Rayl wire mesh	0.3	120, 130, 140
GYREX2	2	None	0.0	120, 130, 140
GYREX2	2	None	0.0	120, 130, 140
GYREX2	2	3cgs Rayl wire mesh	0.3	120, 130, 140
GYREX3	3	None	0.0	120, 130, 140
GYREX3	3	None	0.0	120, 130, 140
GYREX3	3	3cgs Rayl wire mesh	0.3	120, 130, 140
GYREX4	4	None	0.0	120, 130, 140
GYREX4	4	None	0.0	120, 130, 140
GYREX4	4	3cgs Rayl wire mesh	0.3	120, 130, 140

test matrix includes thirty-six configurations, this report focuses on a representative subset to illustrate key findings.

Attenuation over the frequency range is evaluated to understand the performance of these liner samples in a grazing incidence environment. By combining microphone SPL, phase, and microphone locations, the incident and reflected sound pressure levels upstream and downstream of the liner sample can be determined. A simple measurement of liner attenuation is computed by subtracting the pressure levels of the waves traveling with the flow. Details of this method are developed at NASA Langley and will be described in an upcoming publication [16].

3. RESULTS AND DISCUSSION

3.1. Normal Incidence Absorption Results

In our previous study, normal incidence measurements revealed that elongating the gyroid structure has a significant influence on the absorption characteristics, as illustrated in Figure 2. When comparing the base gyroid structures with those elongated along the x-direction, it is clear that elongation increases the magnitude of the absorption peaks and shifts them toward lower frequencies. Specifically, for ρ = 40%, the absorption peak of 0.6 at 1650 Hz for EX1 is shifted to 0.65 at 1450 Hz, 0.67 at 1300 Hz, and 0.73 at 1250 Hz for EX2, EX3, and EX4, respectively. Additionally, the absorption peaks narrow as the elongation factor increases. Notably, the transition from an elongation factor of 2 (EX2) to 3 (EX3) produces a more pronounced effect on both the absorption magnitude and the frequency shift than the change from 3 (EX3) to 4 (EX4), suggesting that there may be a practical limit to the benefits of further elongation.

These encouraging results under normal incidence conditions provide a strong rationale for extending our investigation into more realistic, grazing incidence environments. Since practical applications, such as acoustic liners in aircraft engines, often involve sound waves striking surfaces at oblique or grazing angles and under flow conditions, it is essential to determine whether the enhancements achieved through elongation can be translated into these more complex environments. The remainder of this study focuses on evaluating the acoustic performance of the same elongated gyroid structures under grazing incidence conditions, using the GFIT. By comparing the grazing incidence data with our earlier normal incidence observations, we aim to establish the potential benefits and limitations

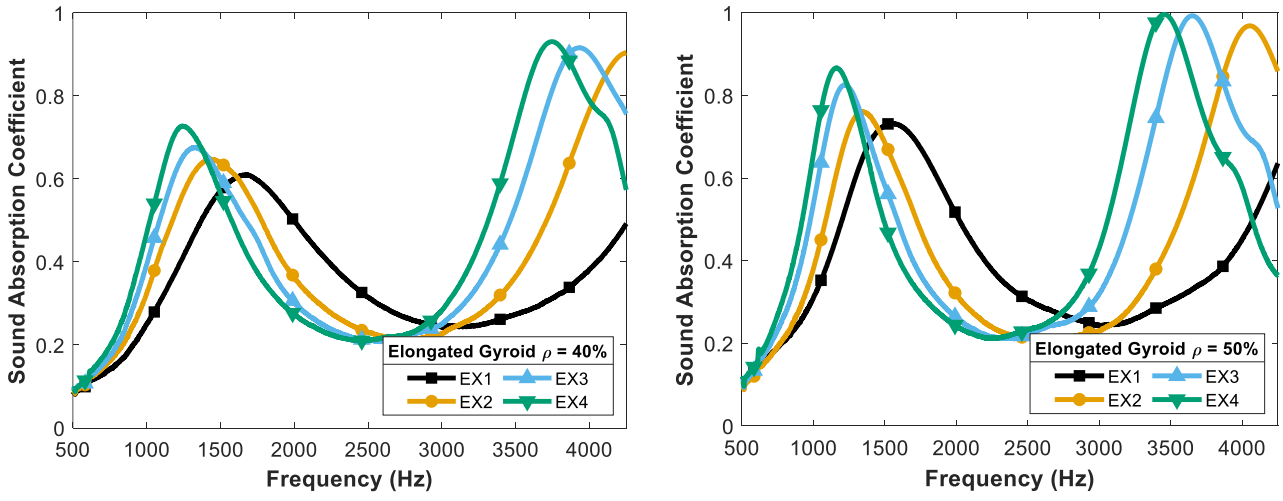

(a) (b)

Figure 2: Normal incidence sound absorption coefficient measurements of elongated gyroid samples with (a) ρ = 40% and the elongation axis chosen to be perpendicular to the sound waves, (b) ρ = 50% and the elongation axis chosen to be perpendicular to the sound waves.

of geometric asymmetry when applied to aeroacoustic environments.

3.2. Acoustic Liner Linearity

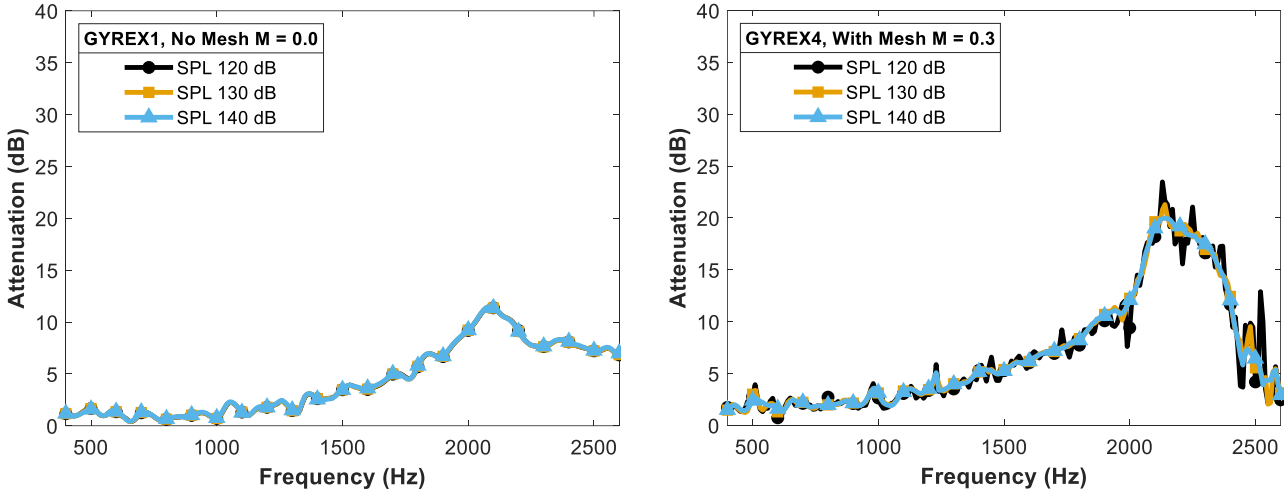

(a) (b)

Figure 3: Comparison of grazing incidence sound attenuation at varying source SPLs for (a) GYREX1 with no mesh, M = 0.0 and (b) GYREX4 with mesh, M = 0.3.

An important initial step in characterizing acoustic liner performance is determining whether the liner's acoustic behavior varies with changes in the SPL. A liner exhibiting acoustic performance independent of SPL is considered linear. Figure 3 illustrates the attenuation spectra for selected configurations to assess linearity. Specifically, Figure 3(a) presents attenuation results for the GYREX1 sample tested without mesh at Mach 0.0 for SPLs of 120, 130, and 140 dB. The resulting curves closely overlap, confirming linear acoustic behavior. Similar trends were observed for other no-flow configurations; therefore, Figure 3(a) is representative of no-flow performance conditions.

Figure 3(b) depicts the attenuation performance of the GYREX4 sample with mesh at Mach 0.3 under identical SPL conditions (120, 130, and 140 dB). The attenuation curves remain largely consistent, suggesting predominantly linear behavior under grazing flow conditions. Similar acoustic performance was observed for the other test samples, with and without flow. Therefore, these samples can be classified as linear.

3.3. Effect of Wire Mesh and Addition of Flow

The influence of incorporating a wire mesh and introducing controlled airflow is clearly illustrated in Figure 4. In Figure 4(a), the results for the GYREX1 (no elongation) sample at 140 dB SPL show that considerable attenuation is achieved above 1600 Hz. In this configuration, the introduction of a wire mesh alone produces only marginal changes compared to the baseline no-mesh, no-flow case. However, when a grazing airflow at Mach 0.3 is applied, the attenuation near the peak frequency of 2300 Hz improves by roughly 7 dB, although this enhancement is largely confined to the frequency range between 2100 and 2500 Hz. In contrast, Figure 4(b) for the more elongated GYREX4 (elongation factor of 4) sample demonstrates a more dramatic response to airflow; here, the peak attenuation at 2300 Hz is enhanced by nearly 15 dB compared to the static condition. It is noteworthy, however, that this significant improvement is accompanied by a sharp drop in attenuation in the 2400–2600 Hz band, indicating a trade-off in the acoustic performance that may be attributed to complex interactions between the geometric modifications and the flow environment.

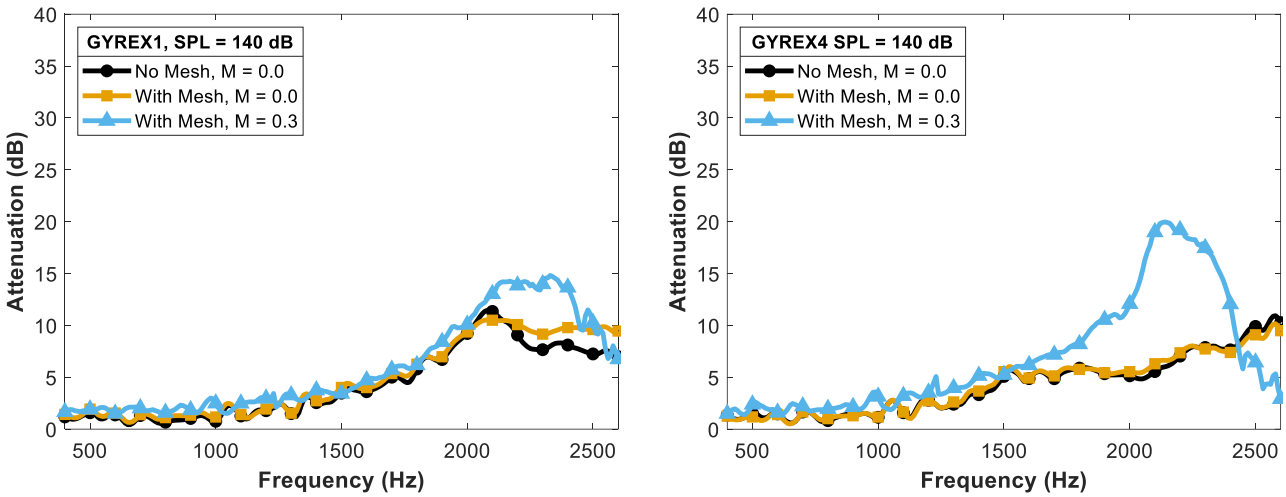

(a) (b)

Figure 4: Effect of test configurations on the grazing incidence sound attenuation for representative examples (a) GYREX1 at source SPL of 140 dB (b) GYREX4 at source SPL of 140 dB.

3.4. Effect of Elongation on the Grazing Incidence Acoustic Attenuation

The effect of elongation on acoustic attenuation is further elucidated in Figure 5. For frequencies below approximately 1800 Hz (Figure 5(a)), the different samples—whether elongated or not—exhibit similar attenuation characteristics, suggesting that the elongation has little impact on the low-frequency response. Another hypothesis is that the samples are too thin to absorb sound at these lower frequencies. In future investigations, thicker samples will be explored. In the intermediate frequency range between 1800 and 2300 Hz, the non-elongated configuration (EX1) displays marginally higher attenuation compared to the elongated cases, with all elongated variants showing very similar behavior. Beyond 2300 Hz, the benefits of elongation become more pronounced. At a source SPL of 140 dB, in the no-mesh, no-flow condition (Figure 5(a)), the sample with an elongation factor of 2 (EX2) attains the highest attenuation, which is observed around 2600 Hz. In contrast, the EX3 and EX4 samples, which are subjected to further elongation, exhibit a modest reduction in highest attenuation. When a mesh is incorporated (Figure 5(b)), these trends persist, and little to no change in attenuation is apparent. The introduction of grazing airflow (Figure 5(c)) results in dramatic improvements in attenuation beyond 2300 Hz. For instance, the non-elongated EX1 sample reaches a peak attenuation of only 15 dB at 2250 Hz, whereas the EX2, EX3, and EX4 samples achieve peak attenuations of approximately 25 dB at 2400 Hz, 25 dB at 2250 Hz, and 20 dB at 2200 Hz, respectively. Similar trends are observed at other SPLs.

These results are consistent with our previous normal incidence findings, in which elongation shifted the absorption peaks toward lower frequencies and enhanced the peak magnitudes. Specifically, the peak frequency shifts of 150 Hz between EX1 and EX2, 150 Hz between EX2 and EX3, and 50 Hz between EX3 and EX4 align well with the peak frequency shifts seen for normal incidence conditions. Although the improvements under grazing incidence are somewhat less dramatic than under normal incidence, the observed trends confirm that geometric asymmetry has a positive influence on acoustic performance even under flow conditions.

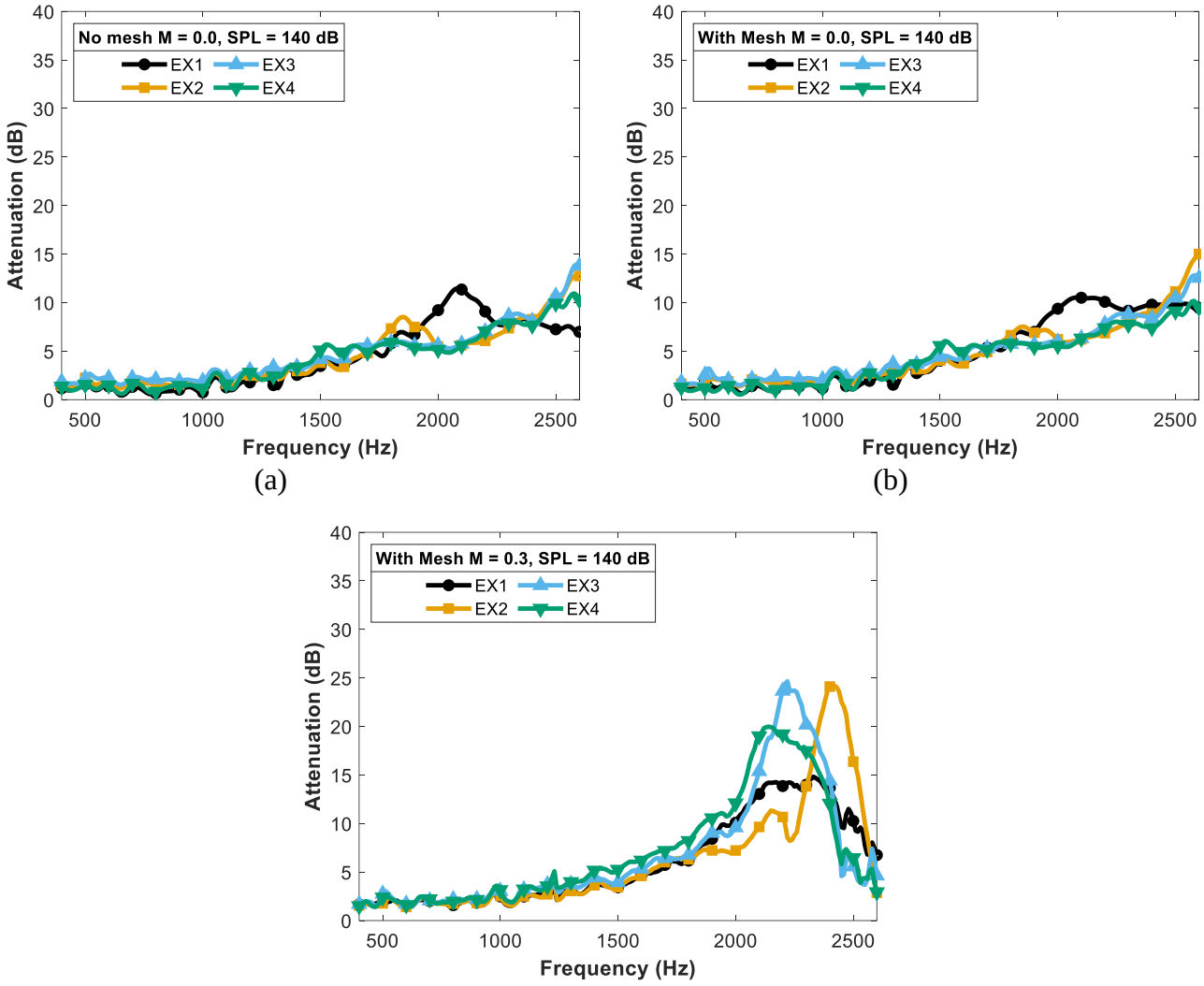

Figure 5: The effect of varying elongation on grazing incidence acoustic attenuation for (a) no mesh, no flow configuration, (b) with mesh, no flow configuration, and (c) with mesh, M = 0.3 flow configuration at 140 dB.

4. CONCLUSIONS

In this study, we expanded upon our prior research on enhancing sound absorption in gyroid TPMS structures through symmetry modifications, focusing specifically on their acoustic behavior under realistic grazing incidence conditions. By fabricating elongated TPMS samples using fused deposition modeling and evaluating their acoustic response within a grazing incidence aeroacoustic setup, we aimed to determine whether the promising results observed under normal incidence conditions would persist when subjected to grazing sound incidence and airflow.

The grazing incidence experiments demonstrate consistent absorption trends across the frequency range for sound pressure levels (SPLs) from 120 to 140 dB, highlighting the linear behavior and SPL independence of the TPMS absorbers. Below 1800 Hz, the elongated and non-elongated samples exhibit similar attenuation characteristics across all configurations, indicating minimal influence of elongation at these lower frequencies. Adding a wire mesh atop the samples caused negligible changes, suggesting

a minor impact of the mesh on sample response. Without airflow, differences between elongated and non-elongated samples remained minimal outside of the frequency band of their peak regions.

However, introducing grazing airflow at Mach 0.3 significantly improved acoustic attenuation above 2300 Hz. At 140 dB, elongated samples EX2, EX3, and EX4 reached peak attenuations of approximately 25 dB, 25 dB, and 20 dB respectively, compared to only 15 dB for the non-elongated EX1 sample. Furthermore, a noticeable shift in peak attenuation toward lower frequencies occurred as elongation increased, consistent across all tested SPL conditions. These observations corroborate our previous normal incidence findings, confirming that introducing geometric asymmetry through elongation shifts absorption peaks to lower frequencies and enhances peak attenuation magnitudes. Although the enhancements under grazing incidence conditions are somewhat less pronounced than those observed at normal incidence, the results validate that geometric asymmetry positively impacts acoustic performance, particularly in the presence of grazing flow.

These findings underscore the potential benefits of introducing geometric asymmetry in TPMS structures for improved acoustic performance under grazing incidence conditions. They provide foundational insights for future research aimed at optimizing design parameters across varied environmental scenarios. Specifically, future investigations will explore elongation directions perpendicular to the flow, at intermediate angles, and in the depth-wise direction. Additionally, future studies will consider thicker sample depths to amplify the effects of geometric modifications and explore their potential to further enhance acoustic performance.

ACKNOWLEDGEMENTS

The authors would like to acknowledge the faculty startup funds received from Michigan Technological University and the liner physics team at the NASA Langley Research Center for their support in Grazing Flow Impedance Testing. This work was funded in part by the Advanced Air Transport Technologies Project of the NASA Advanced Air Vehicles Program.

REFERENCES

[1] A. H. Nayfeh, J. E. Kaiser and D. P. Telionis. Acoustics of aircraft engine-duct systems. *AIAA Journal*, **13(2),** 130-153 (1975).

[2] Y. Qian and J. A. Vanbuskirk. Sound absorption composites and their use in automotive interior sound control. *SAE Transactions*, **104,** 2058-2067 (1995).

[3] W. Yang and J. Y. Jeon. Design strategies and elements of building envelope for urban acoustic environment. *Building and Environment*, **182,** 107121 (2020).

[4] L. Cao, Q. Fu, Y. Si, B. Ding and J. Yu. Porous materials for sound absorption. *Composites Communications*, **10,** 25-35 (2018).

[5] Y. Wu, J. Fang, C. Wu, C. Li, G. Sun and Q. Li. Additively manufactured materials and structures: A state-of-the-art review on their mechanical characteristics and energy absorption. *International Journal of Mechanical Sciences*, **246,** 108102 (2023).

[6] J. Ma, Y. Li, Y. Mi, Q. Gong, P. Zhang, B. Meng, J. Wang, J. Wang and Y. Fan. Novel 3D printed TPMS scaffolds: microstructure, characteristics and applications in bone regeneration. *Journal of Tissue Engineering*, **15,** 1-22 (2024).

[7] X. Yang, Q. Yang, Y. Shi, L. Yang, S. Wu, C. Yan and Y. Shi. Effect of volume fraction and unit cell size on manufacturability and compressive behaviors of Ni-Ti triply periodic minimal surface lattices. *Additive Manufacturing*, **54,** 102737 (2022).

[8] N. Yang, H. Wei and Z. Mao. Tuning surface curvatures and young's moduli of TPMS-based lattices independent of volume fraction. *Materials and Design*, **216,** 110542 (2022).

[9] N. Yang, Z. Qian, H. Wei and M. Zhao. Anisotropy and deformation of triply periodic minimal surface based lattices with skew transformation. *Materials and Design*, **225,** 111595 (2023).

[10] N. Kladovasilakis, K. Tsongas, D. Karalekas and D. Tzetzis. Architected materials for additive manufacturing: a comprehensive review. *Materials*, **15(17),** 5919 (2022).
[11] M. Zhang, C. Liu, M. Deng, Y. Li, J. Li and D. Wang. Graded minimal surface structures with high specific strength for broadband sound absorption produced by laser powder bed fusion. *Coatings*, **13(11),** 1950 (2023).
[12] J. Godakawela, M. Carrillo-Munoz and B. Sharma. Enhancing the absorption performance of minimal surface-based bulk absorbers via symmetry-breaking. *Proceedings of NOISE-CON24*, pp. 837-844. New Orleans, LA (2024).
[13] M. G. Jones, W. R. Watson, D. M. Nark, B. M. Howerton and M. C. Brown. A review of acoustic liner experimental characterization at NASA Langley. NASA/TP–2020–220583 (2020).
[14] Standard Test Method for Impedance and Absorption of Acoustical Materials Using a Tube, Two Microphones and a Digital Frequency Analysis System. ASTM E1050-19, ASTM International, 2019.
[15] B. M. Howerton, H. Vold and M. G. Jones. Application of swept-sine excitation for acoustic impedance eduction. *25th AIAA/CEAS Aeroacoustics Conference*. Delft, The Netherlands (2019).
[16] C. Shoemaker, J. Kreitzman and B. Howerton. Effects of liner length on the educed impedance. *International Forum for Aviation Research*. Las Vegas, NV (2025, to be presented).